Anomalous magneto-transport behaviour near the first order phase transition in $Gd_5Ge_{3.8}Ga_{0.2}$ alloy

2009 J. Phys.: Condens. Matter 21 336007

(http://iopscience.iop.org/0953-8984/21/33/336007)

J. Phys.: Condens. Matter **21** (2009) 336007 (7pp) doi:10.1088/0953-8984/21/33/336007

Anomalous magneto-transport behaviour near the first order phase transition in $Gd_5Ge_{3.8}Ga_{0.2}$ alloy

A Bhattacharyya, S Giri and S Majumdar[1]

Department of Solid State Physics, Indian Association for the Cultivation of Science, 2A&B Raja S C Mullick Road, Jadavpur Kolkata 700 032, India

E-mail: sspsm2@iacs.res.in (S Majumdar)

Received 15 May 2009, in final form 10 July 2009
Published 28 July 2009
Online at stacks.iop.org/JPhysCM/21/336007

Abstract

We study the effect of Ga doping at the Ge site of the metamagnetic compound Gd_5Ge_4. For 5% Ga doping, the resulting alloy ($Gd_5Ge_{3.8}Ga_{0.2}$) shows antiferromagnetic ordering around 130 K, and a thermally driven first order magneto-structural transition at low temperature leading to the ferromagnetic ground state. The alloy shows a noticeable amount of training effect in resistivity when thermally cycled through this first order phase transition (FOPT). The training effect is present in the case of isothermal field cycling. The FOPT region is found to be metastable and extremely sensitive to the applied magnetic field with a clear signature of a metamagnetic transition in the magnetization and resistivity. The metastability is further supported by the large relaxation observed in the resistivity. The giant magnetoresistance observed in the sample is found to be positive near the FOPT, while below the transition it is negative. The resistivity shows irreversibility due to field cycling, which is related to both a field-induced arrested state and some permanent micro-structural changes in the sample.

(Some figures in this article are in colour only in the electronic version)

1. Introduction

In the last decade, the $Gd_5Ge_{4-x}Si_x$ family of intermetallic alloys has attracted considerable attention [1]. This was primarily triggered by the observation of the giant magnetocaloric effect (MCE) in $Gd_5Ge_2Si_2$ in 1997 [2]. These alloys are found to show diverse and fascinating functional properties, which include magnetostriction, giant magnetoresistance, MCE etc. The key to all these functional properties is the magnetic field (H) and/or temperature (T) driven martensitic-type structural transition [3]. The family of materials exhibit many other exotic magnetic and electronic properties, which are of fundamental interest, and they provide an ideal test bed for studying magneto-structural instability in intermetallic systems.

The parent compound Gd_5Ge_4 shows long range antiferromagnetic (AFM) ordering below $T_N \sim 128$ K. Upon the application of H at low-T (<25 K), it undergoes a sharp metamagnetic transition leading to a ferromagnetic (FM) state [4–6]. This is a first order phase transition (FOPT) associated with a change in crystal structure. The ground state of Gd_5Ge_4 is found to be complex with evidence of coexisting phase clusters and kinetically arrested states [7, 8]. With Si doping at the Ge site ($Gd_5Ge_{4-x}Si_x$), the sample shows a T-driven FOPT in zero field from an AFM to an FM state [9–11]. For small Si doping ($x \leqslant 0.8$), both the structures have orthorhombic symmetry, however, they differ by the existence of dimerization between [$Gd_5(Si, Ge)_4$] slabs. While the low temperature FM phase has a Gd_5Si_4-type orthorhombic O(I) structure with covalent Ge(Si)–Ge(Si) bondings, the high temperature AFM/paramagnetic phase has a Sm_5Ge_4-type O(II) structure without such bondings [1]. The AFM to FM transition in $Gd_5Ge_{4-x}Si_x$ is extremely sensitive to H, the composition and the external pressure (P) [9, 12–14], which is the origin of the various functional properties of these alloys. The FOPT, regardless of being triggered by H, P or T, results in very similar crystallographic changes in the system [12].

Some of the Ge-rich compositions of the $Gd_5Ge_{4-x}Si_x$ family show a training effect when thermally cycled through

[1] Author to whom any correspondence should be addressed.

the FOPT. It has been observed that the resistivity (ρ) of the sample increases gradually with the number of thermal cycles. This cycling effect is associated with the tremendous amount of elastic strain that develops during the non-diffusive martensitic transformation (MT). The observed change in ρ with cycling is believed to be related to the stress-induced development of disorder (in the form of micro-cracks) and/or redistribution of Si and Ge atoms causing an intrinsic change in the electronic properties [15–17].

A possible reason for the thermally driven structural instability and simultaneous occurrence of an FM ground state in $Gd_5Ge_{4-x}Si_x$ is the smaller covalent radius of Si as compared to Ge, which in effect exerts a positive chemical pressure [18]. Doping with tetra-valent Si at the Ge site does not change the overall electron to atom ratio (e/a ratio) of the sample. Apart from Si, it has been found that the Gd_5Ge_4 structure remains stable even for small doping with a trivalent ion such as Ga [19]. At room temperature, $Gd_5Ge_{4-x}Ga_x$ ($0 \leqslant x \leqslant 0.6$) alloys are reported to form with an orthorhombic O(II) structure. From the electronic point of view, Ga substitution can be quite different compared to Si, as it changes the e/a ratio of the sample (it has only one 4p electron as compared to two in case of Ge), and it actually has a slightly bigger covalent radius than that of Ge. In the present work we report the detailed magneto-transport studies of a 5% Ga-doped Gd_5Ge_4 sample ($Gd_5Ge_{3.8}Ga_{0.2}$). Despite the contrasting nature of Si and Ga, the studied Ga-doped alloy shows a striking similarity with the similarly Si-doped compositions.

2. Experimental details

The polycrystalline $Gd_5Ge_{3.8}Ga_{0.2}$ sample was prepared by arc melting elemental Gd (99.9 wt% purity), Ge (99.999 wt% purity) and Ga (99.9995 wt% purity) in the stoichiometric ratio under a high-purity argon atmosphere. The as-cast sample was used for the experimental investigation. The sample was characterized by powder x-ray diffraction (XRD) on a Bruker AXS diffractometer using Cu Kα radiation. The XRD pattern signifies an orthorhombic [O(II)] crystal structure, identical to the parent Gd_5Ge_4 compound at room temperature. No impurity phases were detected, and the lattice parameters are found to be $a = 7.67(7)$ Å, $b = 14.73(6)$ Å, and $c = 7.78(1)$ Å for the O(II) structure. The lattice volume is slightly bigger than that of the parent Gd_5Ge_4 compound reported in the literature. The retention of an O(II) structure for small Ga doping in Gd_5Ge_4 and the increase of lattice volume (for $x \leqslant 0.5$) have been reported earlier by Mozharivsky *et al* [19]. The magnetic and transport measurements on the present sample were performed on a commercial cryogen free high magnetic field system from Cryogenic Ltd, UK, fitted with a vibrating sample magnetometer and four probe resistivity options. In all the isothermal measurements, T was stable within 30 mK.

3. Results

The T dependence of magnetization (M) of the $Gd_5Ge_{3.8}Ga_{0.2}$ sample is depicted in figure 1(a). The M–T data, recorded

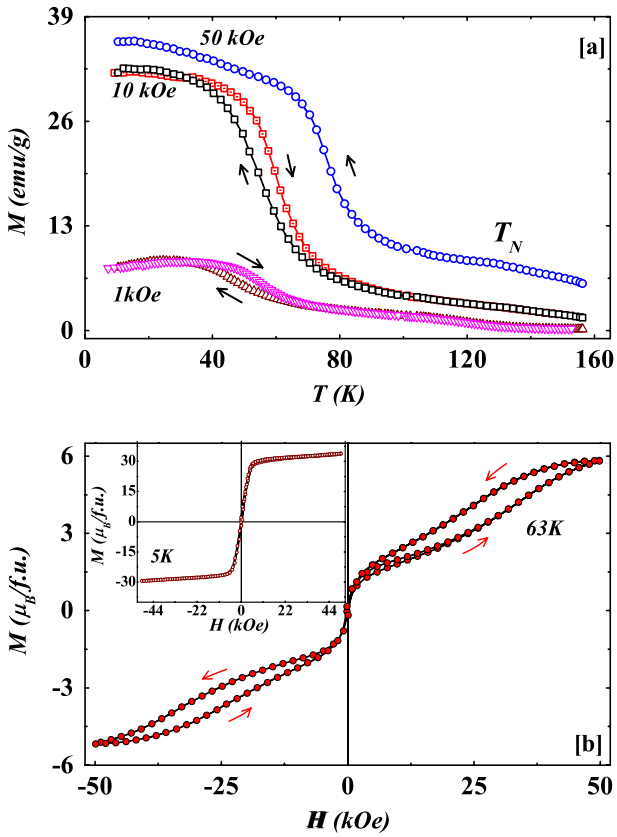

Figure 1. (a) Magnetization is plotted as function of temperature for different applied magnetic fields. For 1 and 10 kOe data for both the field cooling and field heating branches are shown (indicated by arrows). (b) Shows the isothermal magnetization as a function of the applied field at 63 K along with the 5 K isotherm in the inset.

at different H, show a weak hump-like feature around 128 K. Comparing this to the pure Gd_5Ge_4 sample, this feature can be identified as the signature of long range AFM ordering in the sample. Below about 80 K, the sample shows a rise in M, followed by a tendency for saturation at lower T. Clear thermal hysteresis is observed across this transition. The isothermal M–H data recorded at 5 K (see the inset of figure 1(b)) show a predominantly FM character, with a sharp rise at lower fields and a tendency for saturation at higher fields. The anomaly below 80 K can be identified as an FOPT which marks the transition of the high-T AFM phase into the low-T FM phase. The M versus T data for $Gd_5Ge_{3.8}Ga_{0.2}$ indicate that the FOPT below 80 K is highly field sensitive. The transition shifts to higher T with an increasing value of H. We measured the variation of isothermal M with H within the FOPT region ($T = 63$ K). The 4-quadrant $M(H)$ curve has vanishing coercivity near $H = 0$. However, above $H = 5$ kOe, the curve shows a clear change in slope and the increasing and decreasing legs bulge out to form a loop. The loop is found to be symmetric (except the virgin leg) in positive and negative quadrants. This is a clear signature of field-induced metamagnetism, where *AFM phase transforms into FM phase* under H.

Now let us look at the $\rho(T)$ behaviour recorded below 300 K (figure 2(a)). The FOPT observed in $M(T)$ is clearly

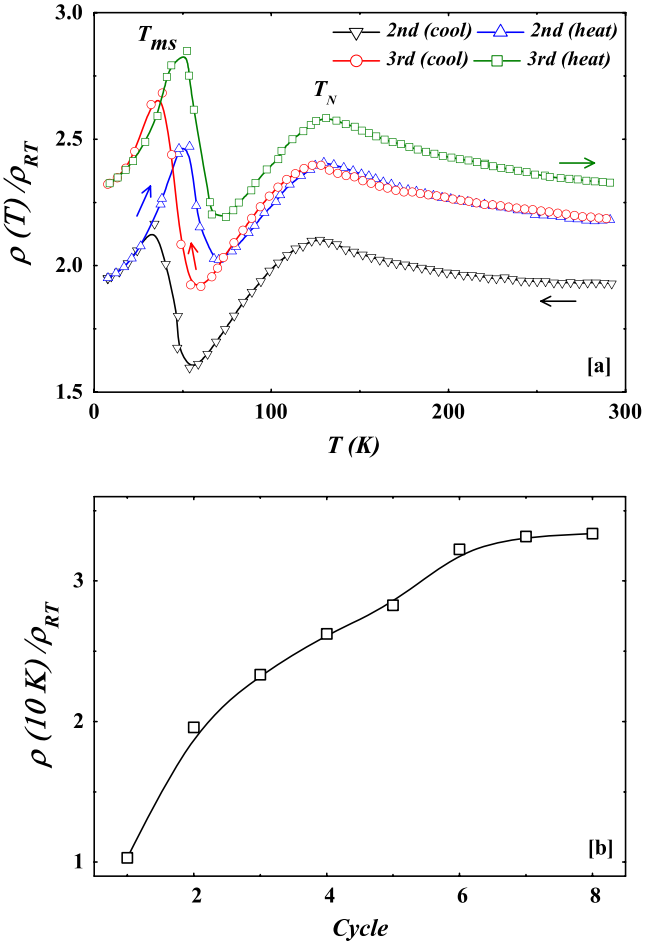

Figure 2. (a) Normalized resistivity of $Gd_5Ge_{3.8}Ga_{0.2}$ is plotted as a function of temperature showing both heating and cooling branches. The thermal cycling for two consecutive runs (2nd and 3rd) are shown, which depicts the thermal cycling effect in the transport data. (b) Normalized resistivity at 10 K for the sample is plotted as a function of the cycling number. The data is normalized with respect to the room temperature value of resistivity (ρ_{RT}) of the uncycled sample.

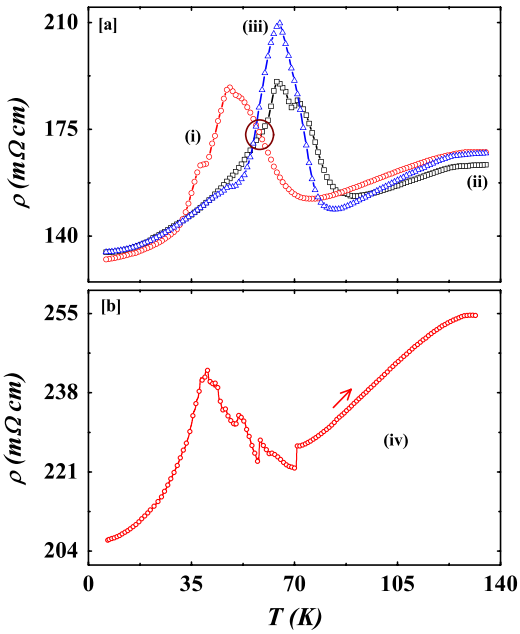

Figure 3. (a) Temperature dependence of resistivity of $Gd_5Ge_{3.8}Ga_{0.2}$ in different magnetic field protocols, namely (i) heating in zero field, (ii) heating in 50 kOe after being field cooled in the same field (iii) cooling in 50 kOe. (b) Shows the zero field heating data after the sample being field cooled in 50 kOe (iv).

visible in the form of a peak in $\rho(T)$, which is denoted by T_{ms}. The paramagnetic to AFM transition is denoted by T_N. Notably, the anomaly near T_N is quite prominent in $\rho(T)$ as compared to that in $M(T)$. The thermal hysteresis in the transition is apparent from the curve: the peak during cooling occurs at 35 K, while during heating it occurs around 50 K. In addition, the peak height at the transition point is higher in the heating data as compared to the cooling data. The hysteresis closes below 30 K toward the low-T end. Unlike a conventional FOPT, the hysteresis in the high-T side is open ended due to the presence of a strong thermal cycling effect. However, this is not present in the M–T data, where the hysteresis loop closes at both ends (see figure 1(a)). ρ systematically increases as it is cycled through the transition. Figure 2(a) shows the data for the second and third cycles (both heating and cooling) and it is clearly seen that in the third cycle the sample has acquired a higher resistance than it had during the second cycle. However, no noticeable change in the transition temperature is observed within the accuracy of measurement. We performed several cyclings on the sample, and the corresponding zero field $\rho(T)$ was measured. Figure 2(b) shows the variation of the value of normalized ρ at 10 K with the cycling number. It is clearly seen that initially ρ increases quite sharply, and subsequently the increase becomes slower.

We measured ρ versus T data in the presence of a field as shown in figures 3(a) and (b). The measurements were performed in different protocols, namely (i) heating in zero field after being cooled in zero field (ZFH) (ii) heating in 50 kOe after being cooled in 50 kOe (FH), (iii) cooling in 50 kOe (FC), and (iv) cooling in 50 kOe and subsequent heating in zero field (FCZFH). In the presence of the T-cycling effect, the actual value of the magnetoresistance $[MR = (\rho(H) - \rho(0))\rho(0)]$ is difficult to estimate from the present $\rho(T, H)$ data. However, several points can be noted. The peak in $\rho(T)$ near the FOPT shifts to higher T with the application of H (compare the two heating data: ZFCH and FCH). However, the magnitude of ρ at the peak remains almost the same. In effect, the sample shows positive MR above a crossing point (marked by a circle in figure 3(a)), while MR is negative below the crossing point. The maximum positive MR (with $H = 50$ kOe) obtained from two consecutive cycles is about 63% (around 63 K), while the maximum negative MR is −27% (around 47 K). This MR contains both the effect of applied field and thermal cycling. Between two cycles, the average increase in ρ is found to be about 14%, so the net effect of field on ρ is reasonably large. We observed step-like avalanches in $\rho(T)$, which are prominent in the measurement protocol (iv) of figure 3(b). Similar avalanches have been observed in many other systems around the first order magneto-structural transition [20, 21].

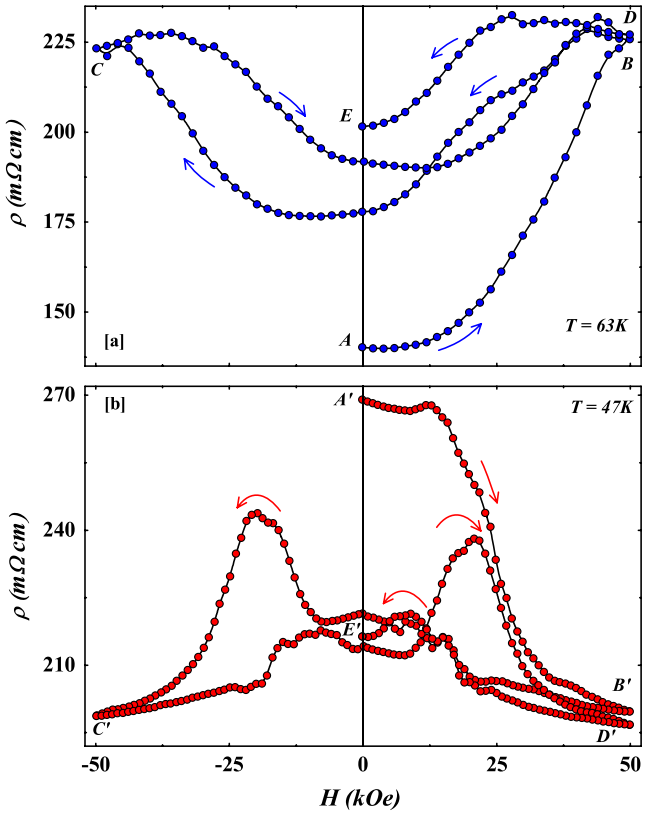

Figure 4. (a) and (b) Show resistivity as a function of the magnetic field for $Gd_5Ge_{3.8}Ga_{0.2}$ recorded at 63 K and 47 K respectively.

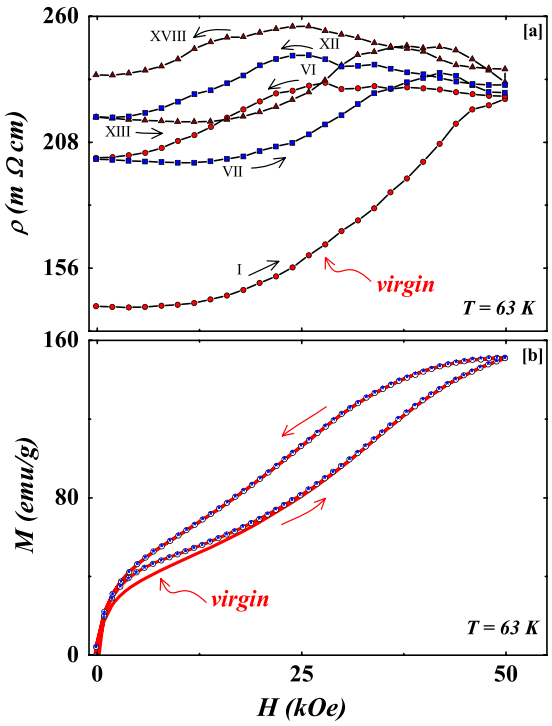

Figure 5. (a) Resistivity is plotted as a function of applied magnetic field at 63 K. The plot depicts three consecutive six-quadrant field cycles. However, for clarity, we show the 1st and 6th legs of each cycle only. The leg numbers are denoted by Roman numerals. (b) Shows the magnetization as a function of the applied field for three consecutive field cycles (they are actually indistinguishable).

Figure 4 shows isothermal ρ versus H data at 63 and 47 K (above and below the crossing point of figure 3(a)). The application of H has a contrasting effect: while ρ increases with H at 63 K indicating positive MR, at 47 K only negative MR is observed. This is due to the fact that these isotherms are recorded on both sides of the crossing point mentioned earlier. The ρ versus H isotherms show clear hysteresis between the increasing and decreasing field legs, in line with the first order nature of the transition. At both the temperatures, strong irreversibility in ρ is observed on field cycling. Clearly after tracing a six-leg cycle between ± 50 kOe, ρ does not come back to its original zero field value. The irreversibility in the field cycling, particularly in a sample with field-induced FOPT, can be due to the arrested magnetic state arising from the metastability associated with the FOPT [22]. For example, we have recently observed a similar open ended $\rho(H)$ loop in cases of a Ni–Mn–Sn based shape memory alloy [23]. For the present $Gd_5Ge_{3.8}Ga_{0.2}$ sample, the effect of H-cycling is much more complex. The traced path has entanglements with several crossing points. The initial application of field produces a large effect on ρ (line AB and $A'B'$ in figures 4(a) and (b) respectively). After this virgin leg, a subsequent change in H produces a relatively smaller effect on the value of ρ (line $BCDE\cdots$), although clear field-hysteresis is present in those subsequent cycles. The ρ versus H curves are not exactly symmetric and regular for positive and negative H. For the 47 K isotherm, ρ shows a peak on the field increasing branch, which is present for both quadrants of H. This peak is less visible in the virgin leg, but becomes very prominent in the subsequent legs. A sharp and non-monotonous change in ρ along with loops for H cycling reflects the field-induced transition in the sample.

In order to shed more light on the H cycling effect, we recorded three consecutive six-leg ($0 \rightarrow 50$ kOe $\rightarrow 0 \rightarrow -50$ kOe $\rightarrow 0 \rightarrow 50$ kOe $\rightarrow 0$) cycles keeping T constant at 63 K. For clarity, we show the first ($0 \rightarrow 50$ kOe) and sixth (50 kOe $\rightarrow 0$) legs of each six-leg cycles in figure 5(a), all of them occur in the positive H quadrant. It is clearly seen that ρ gradually increases with field cycling as well (look at the end points of the loops near $H = 0$). This once again indicates the equivalence of H and T cycling around T_{ms}. We also performed similar cycling measurements in M (see figure 5(b)). The M–H loops at 63 K in the zero-field-cooled state are symmetric in the positive and negative quadrants except for the virgin leg (we show the data in the positive H quadrant only for clarity). The virgin leg stays outside the loop, indicating the H-induced transformation in the system. Unlike $\rho(H)$, the subsequent $M(H)$ legs follow the same path in several cycles of measurements. This clearly indicates that the field cycling effect in $\rho(H)$ after the virgin leg is predominantly connected to micro-structural changes, which have little effect on M.

This equivalence between T and H cycling is further evident from the $\rho(H)$ data recorded on the same sample piece, but with a different thermal cycling history. In figure 6, two zero-field-cooled 63 K isotherms (C_1 and C_2) are shown.

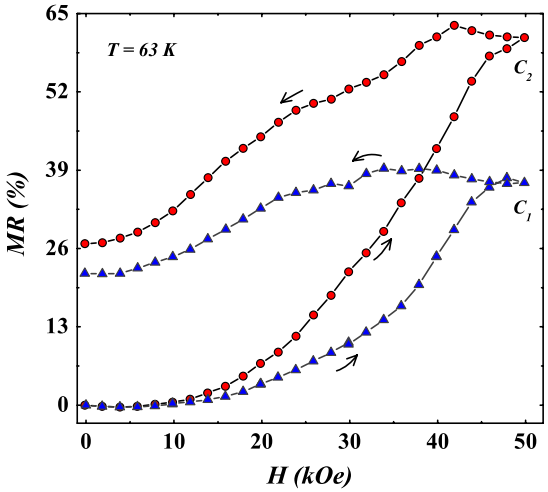

Figure 6. Magnetoresistance (MR) is plotted as a function of applied field at 63 K for $Gd_5Ge_{3.8}Ga_{0.2}$. The two different loops (C_1 and C_2) were recorded on the same piece of sample, but with a different history of thermal and field cycling (see text for details).

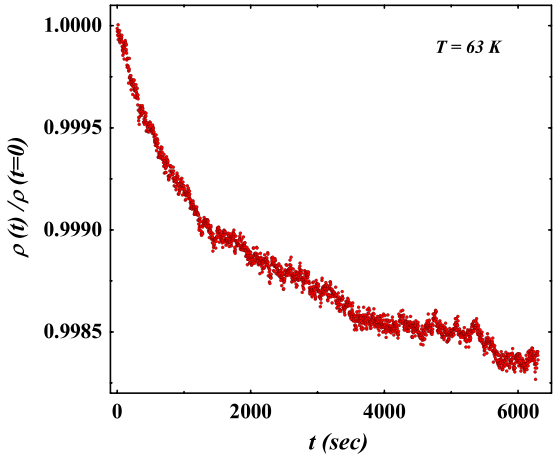

Figure 7. Normalized resistivity is plotted as a function of time for $Gd_5Ge_{3.8}Ga_{0.2}$ at 63 K. The sample was first zero-field-cooled to 63 K, and then 50 kOe of field was applied for two hours. Finally the relaxation was measured by removing the 50 kOe field.

Between C_1 and C_2, the sample was thermally cycled around T_{ms} five times. It is clearly seen that the thermal cycling has a drastic effect on the value of MR: the magnitude of MR has reduced substantially in the isotherm C_2. The MR depends on the electronic transport path, and it gets influenced by *less intrinsic* parameters, such as grains, grain boundaries, defects, disorder etc. The micro-structural changes produced by cycling can therefore act upon the absolute MR of the sample.

Considering the fact that metastable states are produced by the application of H, we recorded the time (t) evolution of ρ as depicted in figure 7. Here the sample was (i) zero-field-cooled to 63 K, (ii) 50 kOe field was applied for a sufficient time (two hours), and (iii) the field was removed and subsequent relaxation of ρ was measured. The data show a visible signature of relaxation (about 0.15% in 6000 s). The relaxation does not follow a simple logarithmic nature, rather it indicates a change in slope around $t = 1500$ s, followed by a sluggish fall. We observe several other small signatures of slope change and jumps, which are visible within the noise level of measurement. The observed relaxation indicates the metastability in the system, which is created by the field-induced arrest around T_{ms}.

4. Discussion

The key observation in the present study is that a very small Ga doping at the Ge site of Gd_5Ge_4 can destabilize the AFM ground state of the system leading to a T-driven FOPT associated with an AFM to FM transition. A previous structural investigation on Ga-doped samples supports our findings by virtue of the fact that beyond $x \geqslant 1.2$ of doping, the alloys assume the Gd_5Si_4 type O(I) structure at room temperature, and this O(I) structure is linked with the ferromagnetism of Gd_5T_4 (T = Si, Ge). However, it will be difficult to predict the actual crystallographic change that takes place at T_{ms} for the present sample. The reported Ga-doped Gd_5Ge_4 samples are found to have three different crystallographic structures (O(II), O(I) or Pu_5Rh_4-type) at room temperature depending on the extent of doping. It might be logical to predict that the transition at T_{ms} is either O(II) $\rightarrow$ O(I) or O(II) $\rightarrow$ Pu_5Rh_4-type. However, this can only be confirmed by XRD measurements at low temperature ($T < T_{ms}$), which is beyond the scope of the present work.

Unlike Si-doped samples, a small amount of Ga doping ($x \leqslant 0.5$) actually expands the lattice volume. This is observed in our sample as well as in a previous report [19]. Therefore, the structural instability leading to an FM ground state cannot simply be explained by the positive chemical pressure effect. The more likely scenario is the change in the electronic concentration when Ge is replaced by Ga. It has been argued that Ge with two 4p electrons favours inter-slab antibonding states in Gd_5Ge_4 and consequently hinders the dimerization between [Gd_5Ge_4] slabs. On the other hand Ga, which has only one 4p electron (henceforth being less electronegative than Ge), weakens the antibonding state and facilitates inter-slab interactions [19]. The inter-slab bonding strengthens the hybridization between the 4p level (of the Ge or Ga atoms) and the 5d level (of the Gd atoms), which favours an FM ground state [24, 25]. Therefore, the magneto-structural transition and the associated development of the FM ground state in $Gd_5Ge_{3.8}Ga_{0.2}$ is closely connected to the e/a ratio of the sample. In addition, the effect of substitutional disorder can play an important role in deciding the ground state.

One of the important findings of the present study on $Gd_5Ge_{3.8}Ga_{0.2}$ is its close resemblance to the physical properties with a Si-doped sample. A particular phenomenon is the thermal cycling effect, which is present in the our compound as well as many Ge-rich Si-doped alloys of the Gd_5Ge_4 family. For the Ge-rich compound, there exists a strong competition between the FM and AFM states with different crystal structures. The elastic energy associated with the strain at the FM/AFM interface in the MT can cause permanent micro-structural changes, which in effect alter the

electron-lattice scattering. For the present sample, we do not observe a noticeable change in T_{ms} with cycling, and the observed effect is predominantly unconnected with the change in intrinsic electronic properties. This is supported by the fact that no cycling effect was observed in the M versus T data.

The magnetic and the magneto-transport behaviour of the present sample is simultaneously influenced by both T and H driven FOPT, which together give rise to a complex H–T behaviour. Owing to the first order nature of the transition, one can have supercooled and superheated states, which are responsible for the thermal and field hysteresis. In a polycrystalline sample such as $Gd_5Ge_{3.8}Ga_{0.2}$, the FOPT is driven by the disorder and one can have the coexistence of both FM and AFM phases [26]. The broad region of hysteresis actually denotes the region of phase coexistence.

In the ρ versus H measurements, we observe a strikingly different nature of the isotherms at 63 and 47 K, which can be explained by the difference in the AFM/FM phase fractions. The complex nature of the ρ versus H behaviour cannot be simply connected to a change in spin disorder scattering, as is often observed near a second order phase transition. The H-induced transition plays a crucial role here. When the sample is zero-field-cooled down to 63 K, the system is predominantly AFM. The application of H creates some FM fraction in the AFM matrix. Due to the presence of two phases, the conduction electron suffers excess scattering from the phase boundaries, consequently ρ increases with H. This is supported by the $\rho(T)$ curves measured in the presence of H (figure 3(a)). The broad peak around T_{ms} in $\rho(T)$ actually arises due to FM/AFM phase separation and subsequent enhanced scattering at the phase boundaries. In the presence of H, the peak shifts to a higher value of T, signifying the shifting of the FM/AFM phase separated region to a higher T. This can only be explained by the formation of an H-induced FM fraction in the otherwise majority AFM phase. ρ will therefore increase as the 63 K region comes under the broad peak in the applied H. On the other, 47 K being close to the lower end point of the hysteresis, there will be a majority FM fraction. Under the applied H, the minority AFM will get transformed to FM. This will cause a decrease in ρ by (i) reducing the amount of the phase boundary, and (ii) by enhancing the FM phase fraction, which actually offers less spin disorder scattering than the AFM phase under an applied field. The peak observed in the ρ versus H curve in the subsequent cycles at 47 K is probably due to the initial rearrangements of phase boundaries for smaller applied fields. It should be borne in mind that the scattering from *FM/AFM boundaries is not restricted to spin dependent scattering*, but it also includes electron-lattice scattering, as the coexisting phases can have different crystallographic structures.

The other interesting observation is the anomalous nature of the virgin $\rho(H)$ curve both at 63 and 47 K. The initial application of H in the zero-field-cooled state gives rise to a distinct virgin leg, which remains separated from the subsequent field loops. The same phenomenon is observed in the M–H measurement, where the virgin leg remains outside the subsequent hysteresis loops. This virgin loop effect is actually connected to the field-induced arrested state across the FOPT. It has been observed in many other systems showing magneto-structural transition, such as manganites, doped $CeFe_2$ and ferromagnetic shape memory alloys [22, 23, 27]. Notably, the effect of H on the virgin state of $Gd_5Ge_{3.8}Ga_{0.2}$ comprises an *irreversible* as well as a *reversible* part. The irreversible part remains arrested even when the field is removed, while the reversible part returns back to the zero field value on field removal and changes again on application of H. This is evident from the $\rho(H)$ loops executed on H-cycling after the virgin leg. This is in sharp contrast with the field-induced arrested state reported by our group in Ni-Mn-Sn based alloys [23], where a total arrest was observed with a completely irreversible nature in the $\rho(H)$ virgin curve.

The metastability associated with the field-arrested state is further revealed by the observed relaxation. MT is generally athermal in nature, i.e. it occurs from the change in external parameters only [28]. However, in certain situations, transition can occur between different metastable/stable states by the aid of thermal fluctuations. This is particularly relevant when disorder can locally reduce the free energy barrier. A similar relaxation has been observed in the pure Gd_5Ge_4 compound at low temperature [8].

We found that similar to the T-cycling, the H-cycling causes the magnitude of ρ to increase gradually. Since it does not get reflected in M, the predominant cause of this training effect in ρ is the micro-structural changes. The structural transition induced by H is martensitic in nature and hence a large elastic strain in tandem with the brittle nature of the sample can cause permanent micro-cracks responsible for the ρ enhancement with H-cycling. In this context we would like to mention that the $\rho(H)$ loops have rather a complex structure (to some extend crisscrossed and asymmetric with respect to positive and negative H) as compared to the smooth and symmetric $M(H)$ curve. This is possibly due to the H-driven micro-structural changes, which by their nature will be stochastic.

Another manifestation of the elastic strain associated with the MT is the observed step-like avalanches in ρ (figure 3(b)). Depending upon T or H, one of the phases (FM or AFM) remains metastable. However, the inter-facial strain field tends to hinder the transition to the stable phase. When the system is driven by H or T, a small fluctuation can help the system to overcome the free energy barrier, resulting in the burst-like growth of the stable phase. The largest jumps are observed in $\rho(T)$ in figure 3(b) measured in the FCZFH protocol. Here, the field cooling, and subsequent heating in $H = 0$ makes the FM phase highly metastable, and the stable AFM phase nucleates in the form of avalanches.

In conclusion, we report the observation of an FM ground state in the Ga-doped Gd_5Ge_4 sample, which develops through a magneto-structural transition from a high temperature AFM phase. Unlike the Si-doped sample, the ferromagnetism in the present sample is related to the decrease in valence electron concentration by the replacement of Ge by Ga. The sample shows a training effect in ρ both for T and H cycling, and micro-structural changes developed by the elastic strain appear to be responsible for the gradual increase of ρ with cycling. We observe unusual virgin loop behaviour in the field dependent M

and ρ measurements, which is connected to the field-induced arrested state within the models of FOPT. In a nutshell, the material is an important addition to the family of Gd_5Ge_4-derived alloys with exotic electronic and magnetic properties.

Acknowledgment

A B wants to thank the Council for Scientific and Industrial Research, India for his research fellowship.

References

[1] Pecharsky V K and Gschneidner K A Jr 2001 *Adv. Mater.* **13** 683
[2] Pecharsky V K and Gschneidner K A Jr 1997 *Phys. Rev. Lett.* **78** 4494
[3] Morellon L, Algarabel P A, Ibarra M R, Blasco J, García-Landa B, Arnold Z and Albertini F 1998 *Phys. Rev.* B **58** R14721
[4] Levin E M, Pecharsky V K, Gschneidner K A Jr and Miller G J 2001 *Phys. Rev.* B **64** 235103
[5] Tang H, Pecharsky V K, Gschneidner K A Jr and Pecharsky A O 2002 *Phys. Rev.* B **69** 064410
[6] Hardy V, Majumdar S, Crowe S, Lees M R, Paul D McK, Hervé L, Maignan A, Hébert S, Martin C, Yaicle C, Hervieu M and Raveau B 2004 *Phys. Rev.* B **69** R020407
[7] Perkins G K, Moore J D, Chattopadhyay M K, Roy S B, Chaddah P, Pecharsky V K, Gschneidner K A Jr and Cohen L F 2007 *J. Phys.: Condens. Matter* **19** 176213
[8] Moore J D, Perkins G K, Morrison K, Ghivelder L, Chattopadhyay M K, Roy S B, Chaddah P, Gschneidner K A Jr, Pecharsky V K and Cohen L F 2008 *J. Phys.: Condens. Matter* **20** 465212
[9] Morellon L, Blasco J, Algarabel P A and Ibarra M R 2002 *Phys. Rev.* B **62** 1022
[10] Casanova F, Labarta A, Batlle X, Marcos J, Mañosa L, Planes A and de Brion S 2004 *Phys. Rev.* B **69** 104416
[11] Pecharsky V K, Pecharsky A O and Gschneidner K A Jr 2002 *J. Alloys Compounds* **344** 362
[12] Mudryk Ya, Lee Y, Vogt T, Gschneidner K A Jr and Pecharsky V K 2005 *Phys. Rev.* B **71** 174104
[13] Levin E M, Pecharsky V K, Gschneidner K A Jr and Tomlinson P 2000 *J. Magn. Magn. Mater.* **210** 181
[14] Tseng Y C, Haskel D, Lang J C, Sinogeikin S, Mudryk Ya, Pecharsky V K and Gschneidner K A Jr 2007 *Phys. Rev.* B **76** 014411
[15] Levin E M, Pecharsky A O, Pecharsky V K and Gschneidner K A Jr 2001 *Phys. Rev.* B **63** 064426
[16] Sousa J B, Braga M E, Correia F C, Carpinteiro F, Morellon L, Algarabel P A and Ibarra M R 2003 *Phys. Rev.* B **67** 134416
[17] Sousa J B, Pereira A M, Correia F C, Teixeira J M, Araújo J P, Pinto R P, Braga M E, Morellon L, Algarabel P A, Magen C and Ibarra M R 2005 *J. Phys.: Condens. Matter* **17** 2461
[18] Mudryk Ya, Paudyal D, Pecharsky V K and Gschneidner K A Jr 2008 *Phys. Rev.* B **77** 024408
[19] Mozharivsky Y, Choe W, Pecharsky A O and Miller J C 2003 *J. Am. Chem. Soc.* **125** 15183
[20] Chattopadhyay M K, Manekar M A, Pecharsky A O, Pecharsky V K, Gschneidner K A Jr, Moore J, Perkins K, Bugoslavsky Y V, Roy S B, Chaddah P and Cohen L F 2004 *Phys. Rev.* B **70** 214421
[21] Hardy V, Majumdar S, Lees M R, Paul D McK, Yaicle C and Hervieu M 2004 *Phys. Rev.* B **70** 104423
[22] Chattopadhyay M K and Roy S B 2008 *J. Phys.: Condens. Matter* **20** 025209
[23] Chatterjee S, Giri S, Majumdar S and De S K 2008 *Phys. Rev.* B **77** 012404
[24] Haskel D, Lee Y B, Harmon B N, Islam Z, Lang J C, Srajer G, Mudryk Ya, Gschneidner K A Jr and Pecharsky V K 2007 *Phys. Rev. Lett.* **98** 247205
[25] Paudyal D, Pecharsky V K and Gschneidner K A Jr 2008 *J. Phys.: Condens. Matter* **20** 235235
[26] For a review see Roy S B and Chaddah P 2004 *Phase Transit.* **77** 767
[27] Tokura Y, Kuwahara H, Moritomo Y, Tomioka Y and Asamitsu A 1996 *Phys. Rev. Lett.* **76** 3184
[28] Planes A, Férez-Reche F-J, Vives E and Mañosa L 2004 *Scr. Mater.* **50** 181